

InterAgent: Physics-based Multi-agent Command Execution via Diffusion on Interaction Graphs

Bin Li^{* 1} Ruichi Zhang^{* 2} Han Liang^{† 3} Jingyan Zhang¹ Juze Zhang⁴
 Xin Chen³ Lan Xu¹ Jingyi Yu¹ Jingya Wang^{† 1,5}
¹ ShanghaiTech University ² University of Pennsylvania ³ ByteDance
⁴ Stanford University ⁵ InstAdapt

Abstract

Humanoid agents are expected to emulate the complex coordination inherent in human social behaviors. However, existing methods are largely confined to single-agent scenarios, overlooking the physically plausible interplay essential for multi-agent interactions. To bridge this gap, we propose InterAgent, the first end-to-end framework for text-driven physics-based multi-agent humanoid control. At its core, we introduce an autoregressive diffusion transformer equipped with multi-stream blocks, which decouples proprioception, exteroception, and action to mitigate cross-modal interference while enabling synergistic coordination. We further propose a novel interaction graph exteroception representation that explicitly captures fine-grained joint-to-joint spatial dependencies to facilitate network learning. Additionally, within it we devise a sparse edge-based attention mechanism that dynamically prunes redundant connections and emphasizes critical inter-agent spatial relations, thereby enhancing the robustness of interaction modeling. Extensive experiments demonstrate that InterAgent consistently outperforms multiple strong baselines, achieving state-of-the-art performance. It enables producing coherent, physically plausible, and semantically faithful multi-agent behaviors from only text prompts. Our code and data will be released to facilitate future research. Project page: <https://binlee26.github.io/InterAgent-Page>.

1. Introduction

Humanoid agents should embody the intrinsic ways we human beings interact and communicate with each other, so as to depict the diverse cultures and societies that make up our physical world. Empowering such agents to perform coordinated behaviors in shared environments stands as a core computer vision challenge, with various applications spanning gaming, VR/AR, and autonomous robots.

Recent kinematics-based approaches for human motion

^{*}Equal contribution.

[†]Corresponding authors.

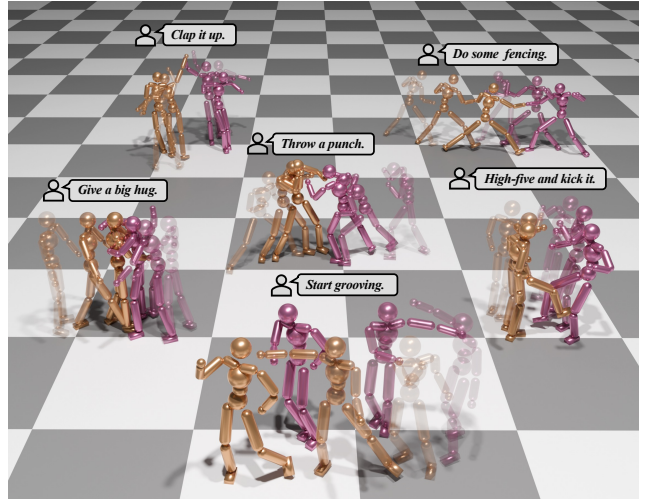


Figure 1. **InterAgent** produces physically plausible multi-agent interactions across diverse scenarios from only text prompts.

generation, empowered by generative models such as diffusion models [2, 16, 32, 55, 74, 81] and autoregressive models [27], have demonstrated promising capabilities in synthesizing interactive motions. Yet, they neglect physical plausibility, often introducing artifacts such as body penetration, floating, or unnatural sliding—significantly compromising both the realism and practical applications. In parallel, the rapid advancement of reinforcement learning and physics simulation has spurred growing interest in physics-based methods [12, 23, 53, 54, 65, 66, 80, 98]. Typically, the generation-and-track frameworks like PhysDiff [96] and CLoSD [65] leverage imitation-learned motion tracking policy to project generated kinematic motions into physically plausible trajectories that minimize tracking error. Yet, they struggle with the inherent discrepancy between kinematic priors and physics-based tracking, often producing unexpected falling movements. Alternatively, recent diffusion policy techniques [6, 51, 78, 86, 100] enables training end-to-end generative policies, such as PDP [66],

UniPhys [80], and Diffuse-CLoC [23]. They form a track-then-distill paradigm, in which a tracking policy is first trained to collect physically plausible state-action trajectories from human motion dataset, which are subsequently used to train generative model as behavior cloner in an end-to-end fashion. Despite their effectiveness, these approaches are predominantly confined to single-agent setting, leaving the rich and complex dynamics of multi-agent interactions—such as collaborative tasks or social-aware behaviors largely underexplored.

To bridge this gap, we introduce InterAgent, a novel physics-based end-to-end framework for text-driven multi-agent humanoid control, which enables producing vivid and physically plausible multi-agent interactions from only text prompts. Specifically, in our multi-agent system, each agent governs its own dynamics through proprioception while perceiving others via exteroception. However, modeling exteroception naively as relative dynamical states overlooks the fine-grained joint-to-joint dependencies crucial for coordinated interactions. To overcome this limitation, we propose to incorporate **interaction graph exteroception** representation into diffusion framework, wherein joints are modeled as nodes interconnected via directed edges. This formulation enables explicit and granular modeling of inter-agent relations. Motivated by the inherent modality heterogeneity among proprioception, exteroception, and action, our Interaction Diffusion Transformer (Inter-DiT) employs a multi-stream architecture that treats each modality as a distinct yet complementary stream. Each **multi-stream DiT block** integrates an inter-stream fusion attention to facilitate cross-modal information exchange, alongside a context-aware conditioning attention that incorporates temporal and inter-agent contextual cues. This design preserves the unique characteristics of each modality while enabling synergistic coordination, thereby achieving a more holistic representation of interaction dynamics. Furthermore, inspired by the sparse and selective nature of real-world human interactions, we introduce a tailored **edge-based sparse attention** mechanism on interaction graph within the exteroception stream. This mechanism dynamically suppresses edges that contribute minimally to the ongoing interaction, thereby focusing the model’s attention on the most salient joint-level dependencies and enhancing the plausibility of synthesized interactions. Extensive experiments demonstrate that our approach consistently outperforms several baselines, generating interactive behaviors that are physically plausible, semantically aligned, and rich in fine-grained coordination.

To summarize, our main contributions include:

- We propose InterAgent, the first end-to-end framework for physics-based text-driven multi-agent humanoid control, achieving state-of-the-art performance.
- We propose Inter-DiT, which incorporates a novel multi-

stream DiT block design that decouples proprioception, exteroception and action modeling, effectively improving the interaction results.

- We propose interaction graph exteroception representation and a tailored sparse edge-based attention mechanism, which further improves the robustness of inter-agent spatial dependencies.

2. Related Work

Physics-based humanoid control. A long-standing goal in computer animation is to design controllers that produce agile and life-like behaviors. Early optimization-based methods [10, 22, 31, 93] explicitly crafted skill-specific objectives but relied on labor-intensive heuristics and lacked generalization. Recent advances increasingly adopt reinforcement learning to learn controllers from data. Many works focus on motion tracking, where policies imitate reference clips [17, 19, 25, 35, 39–41, 46, 58, 70, 71, 79, 94]. Among them, PHC [41] and PULSE [40] scaling tracking to large datasets. Beyond tracking, other studies [47, 48, 72, 89, 101] learn general motion priors from unstructured motion data, enabling agents to compose and adapt skills. Text-conditioned controllers [11, 12, 28, 29, 52, 66, 90] further map language to actions, as in PADL [28] and PDP [66], but remain limited to single-agent scenarios. To move beyond, recent works explore physics-based synthesis of human–object interactions [1, 3, 9, 30, 43, 45, 63, 69, 73, 83, 95], such as InterMimic [84] and CoHIOI [18], enable single-agent skill coordination with dynamic objects but still struggle with complex multi-agent interactions.

Human interaction synthesis. Realistic interaction behaviors, where agents coordinate and respond to each other, have attracted increasing attention. Most approaches are kinematic and data-driven [4, 8, 16, 36, 55, 56, 62, 77, 81, 82, 91, 92], such as InterGen [32] with a diffusion-based text-to-interaction model, and Think-Then-React [61] leveraging large language models for joint intention inference and motion prediction. While effective for semantic alignment, these methods ignore physical feasibility and dynamic interactions. Physics-based approaches [75, 97] produce physically plausible behaviors and capture interaction forces, but remain limited to task-specific settings or rely on a narrow set of reference motions, restricting their ability to model diverse interactive behaviors.

Diffusion models in physics-based humanoid control. Diffusion models [14, 21, 42, 59, 60, 88] have recently emerged as powerful generative frameworks for control, capturing multimodal action distributions and flexible conditioning [5, 7, 23, 26, 50, 57, 64, 67, 96]. CLoSD [65] separates a diffusion motion planner from a tracking controller, while PDP [66] learns an end-to-end diffusion policy for direct control. Diffuse-CLoC [24] and UniPhys [80]

further unify state–action modeling and long-horizon planning. Despite these advances, the existing diffusion-based frameworks are restricted to single-agent control, and the complex multi-agent interaction setting remains unsolved.

3. Preliminaries

Physics simulation setup. We simulate the dynamics of physics-based humanoids [46, 47] in Isaac Gym [33]. Each humanoid agent is equipped with 15 joints and 28 actuators, with each actuator controlled via a proportional-derivative (PD) controller, and the action \mathbf{a}_t specifies the target inputs for its actuators. Given the current states \mathbf{s}_t , the physics simulator advances the humanoids to the next states \mathbf{s}_{t+1} , sampled according to the dynamic transition $\mathbf{s}_{t+1} \sim p(\mathbf{s}_{t+1}|\mathbf{s}_t, \mathbf{a}_t)$.

Interaction tracking policy.

Previous works [40, 41, 46] employ reinforcement learning to replicate MoCap datasets, which effectively imitate the reference motions with a learned tracking policy, $\mathbf{a}_t = \pi(\mathbf{s}_t, \mathbf{s}_{t+1}^{ref})$, where \mathbf{s}_{t+1}^{ref} is the next-frame reference state from reference motions. We adopt a curriculum learning strategy analogous to PHC [41], which progresses from simpler to more complex motions. To faithfully capture the dynamics of inter-agent interactions, we supplement the tracking reward with an interaction graph reward [97]—a design that explicitly enforces the natural spatial relationships between interacting agents.

Data collection. Next, we leverage the trained expert policies to collect state-action trajectories, constituting the tracking dataset. To enhance state space coverage, we augment trajectory diversity by noise disturbance, as introduced in PDP [66]. Specifically, for a given motion sequence $\mathbf{m} = \{\mathbf{s}_t^{ref}\}_{t=1}^n$, we deploy its corresponding tracking policy π in the simulator to roll out diverse trajectories like $\{\mathbf{s}_1, \mathbf{a}_1, \dots, \mathbf{s}_n, \mathbf{a}_n\}$, where $\mathbf{a}_t = \pi(\mathbf{s}_t, \mathbf{s}_t^{ref}) + \epsilon$ with $\epsilon \sim \mathcal{N}(0, \sigma^2)$. Finally, the noisy-state clean-action trajectory $\{\mathbf{s}_1, \pi(\mathbf{s}_1, \mathbf{s}_1^{ref}), \dots, \mathbf{s}_n, \pi(\mathbf{s}_n, \mathbf{s}_n^{ref})\}$, along with the text description associated with the motion sequence \mathbf{m} , are collected into the dataset \mathcal{D} . In practice, to ensure the reliability of the collected data, we perform multiple rollouts for each motion and select 8 successful trajectories as training samples. Empirically, a noise level of $\sigma = 0.01$ strikes a good balance between bandwidth and temporal stability.

4. Method

We focus on physics-based text-driven control for two interacting humanoid agents. In single-agent settings, **actions** depend mainly on an agent’s own state (**proprioception**). In contrast, multi-agent scenarios introduce additional challenges: each agent’s actions are influenced not only by its intrinsic dynamics but also by the other’s states and behaviors (**exteroception**). To this end, we propose a novel

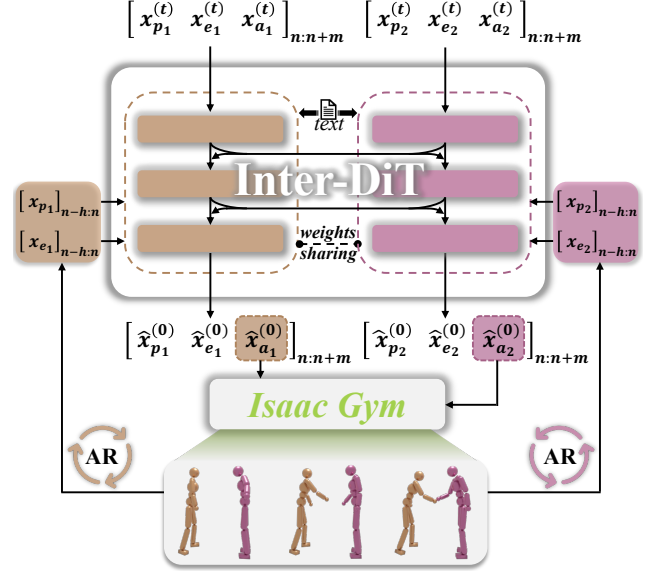


Figure 2. **InterAgent overview.** A physics-based framework for text-driven multi-agent interactive behavior generation, built upon Inter-DiT — two cooperative, weight-sharing networks under an autoregressive diffusion paradigm.

framework InterAgent (Fig. 2). It incorporates an Interaction Diffusion Transformer (Inter-DiT), composed of two cooperative, weight-sharing networks under an autoregressive diffusion paradigm (Sec. 4.1), to effectively model interactive dynamics. Given the inherent heterogeneity among proprioception, exteroception, and action, we treat them as distinct modalities. To handle these modalities in a coordinated manner, Inter-DiT adopts a multi-stream architecture (Sec. 4.2) that enables decoupled yet cooperative modeling and enhances overall performance. Moreover, we propose a novel and effective exteroception representation, interaction graph (IG), and devise a tailored edge-based sparse attention mechanism on the exteroception stream (Sec. 4.3) to selectively suppress interaction-irrelevant connections and effectively highlight salient inter-agent relations, based on its sparsity nature.

4.1. Interaction Diffusion Transformer

We propose the Interaction Diffusion Transformer (Inter-DiT), a novel autoregressive diffusion framework designed to model the interactive behaviors between agents, as illustrated in Fig. 2. Inspired by Diffuse-CLOC [23] and UniPhys [80], we model the joint distribution of states and actions under textual conditions \mathbf{c} , enabling coherent prediction of future state-action pairs with implicitly learned dynamic transition world model.

Humanoid behavior representation. We represent the humanoid behavior sequence as $\mathbf{X} = \mathbf{x}_{1:T} = [\mathbf{x}_s, \mathbf{x}_a]_{1:T}$, where \mathbf{x}_s and \mathbf{x}_a denotes the state and action, respectively.

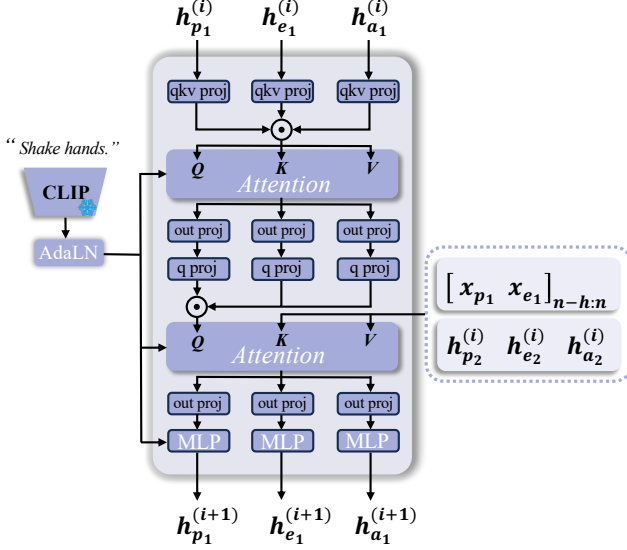


Figure 3. **Multi-stream DiT block design.** Each modality—proprioception, exteroception, and action—is processed in an independent stream. Inter-stream fusion attention exchanges information across modalities, while context-aware conditioning attention integrates temporal and inter-agent context, enabling decoupled yet coordinated modeling.

To be specific, each state x_s is composed of the following elements:

$$x_s = (R_h, \mathbf{p}, \mathbf{r}, \mathbf{v}, \mathbf{w}), \quad (1)$$

where $R_h \in \mathbb{R}$ denotes the heights of the root from the ground. $\mathbf{p} \in \mathbb{R}^{(J-1) \times 3}$ denotes the 3D position of each joint (excluding the root) within the humanoid’s root frame. $\mathbf{r} \in \mathbb{R}^{J \times 6}$ encodes the local rotation of each joint using 6D representation [99]. In addition, $\mathbf{v} \in \mathbb{R}^{J \times 3}$ and $\mathbf{w} \in \mathbb{R}^{J \times 3}$ is the local linear and angular velocities of each joint, respectively. As for each action x_a , it specifies the target joint rotations used by PD controllers to drive the humanoid’s movements. The resulting control signals form a 28-dof action space for each humanoid.

Interaction graph exteroception. In our multi-agent scenarios, the behavior of each agent is inherently influenced by its spatiotemporal interactions with others. To capture such interdependencies, we extend the state representation x_s in Eq. (1) by incorporating an additional exteroception component, yielding $x_s = [x_p, x_e]$, where x_p represents the proprioception (as defined in Eq. (1)) and x_e encodes exteroceptive information reflecting inter-agent interactions. An intuitive design for exteroception modeling is to directly represent the other agent’s proprioception state in the agent’s own root frame, which we refer to as relative state (RS) exteroception.

However, we find that such a naive exteroception representation is suboptimal for learning complex interactive pat-

terns. Drawing inspiration from Zhang et al. [97], we propose the interaction graph (IG) as the exteroception, which provides a more explicit and structured representation of inter-agent dynamics. Specifically, for each joint position $\mathbf{p}_j \in \mathbb{R}^3$ of a humanoid, we construct directed edges towards every joint position $\mathbf{p}_i \in \mathbb{R}^3$ of the other humanoid, where each edge $e_{ij} = \mathbf{p}_i - \mathbf{p}_j \in \mathbb{R}^3$ encodes the spatial interaction between the corresponding joints, as shown in Fig. 4. We refer to this as fully connected IG (FIG) exteroception, written as

$$x_e = (e_{1,1}, e_{1,2}, \dots, e_{J,J}) \in \mathbb{R}^{(J*J) \times 3}, \quad (2)$$

where J denotes the number of joints of one humanoid.

Training and inference. For simplicity, we omit the explicit agent indices and use a single notation to represent both agents. As illustrated in Fig. 2, Inter-DiT models the symmetry of two agents using two cooperative and weight-sharing networks, inspired by InterGen [32]. It takes as input a noisy interaction behavior sequence $\mathbf{X}^{(t)} = [x_p^{(t)}, x_e^{(t)}, x_a^{(t)}]_{n:n+m}$ of length m and output a denoised sequence. The past h frames of proprioception and exteroception, $\mathbf{S} = [x_p, x_e]_{n-h:n}$, serve as historical states over the previous h frames, where n denotes the current frame. Inter-DiT is trained to predict the future behaviors $\hat{\mathbf{X}}^{(0)}$ given all agents’ historical behavior states \mathbf{S} and text condition c in an autoregressive manner. The training objective is defined as:

$$\mathcal{L} = \mathbb{E}_{t, \mathbf{X}} [\|\mathbf{X} - \Phi(\mathbf{X}^{(t)}, t, c, \mathbf{S})\|], \quad (3)$$

where t is the diffusion timestep.

During inference, states from the simulator are stored in a first-in-first-out (FIFO) history buffer. Given a command c , Inter-DiT starts from a noisy sequence, uses the latest h frames as context, and predicts actions \hat{x}_a to drive the humanoids, repeating autoregressively for the desired steps.

4.2. Multi-stream DiT Block

As mentioned, Inter-DiT enables coherent prediction of future state-action pairs. Unlike prior works [23, 80] that merge states and actions into a single representation, we treat them as distinct modalities of behavior to reduce inter-modal interference. In multi-agent scenarios, the proprioception and exteroception should also be considered as separate modalities due to their heterogeneous nature. Motivated by prior works [15, 34, 37, 76], Inter-DiT employs multi-stream blocks to model these distinct modalities as disentangled streams. As depicted in Fig. 3, each multi-stream Inter-DiT block is structured into inter-stream fusion attention and contextual conditioning attention stages.

Inter-stream fusion attention. Firstly, the i -th hidden features of an agent $[h_{p1}^{(i)}, h_{e1}^{(i)}, h_{a1}^{(i)}]$ are independently projected into a shared feature space. Then, the features from

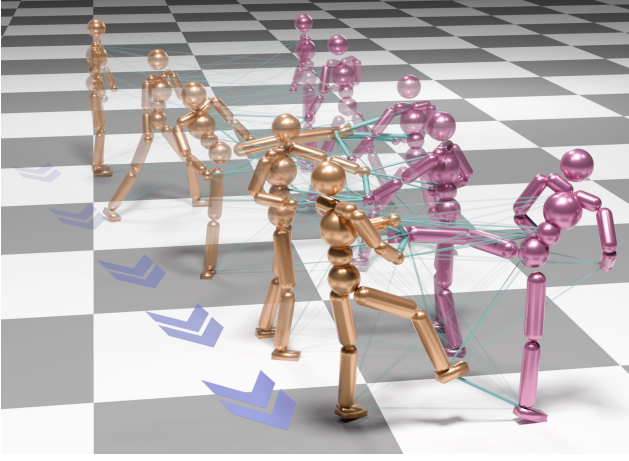


Figure 4. **Sparse Interaction Graph.** Each joint of one character connects to all joints of the other via directed edges (dark green), where each edge vector encodes the spatial interaction between the corresponding joints. The thickness of each edge encodes the magnitude of its contribution to the interactive dynamics. Light purple arrows on the ground indicate temporal progression.

each stream are concatenated along the sequence dimension, and the resulting aggregated features are encoded via self-attention. After attention, the outputs are then split and routed through dedicated projection layers to mitigate inter-modal interference.

Context-aware conditioning attention. To infuse temporal and inter-agent contextual cues, the outputs from all streams of the previous stage are concatenated along the sequence dimension and used as queries. The keys and values are provided sequentially from history observations $[\mathbf{x}_{p_1}, \mathbf{x}_{e_1}]_{n-h:n}$, and the hidden features $[\mathbf{h}_{p_2}^{(i)}, \mathbf{h}_{e_2}^{(i)}, \mathbf{h}_{a_2}^{(i)}]$ of the other agent. After sequentially attending to each contextual cue with a dedicated attention layer [68], the resulting outputs are split and passed through their respective projection layers. Finally, the output of each stream is processed by a feed-forward MLP to yield the $(i+1)$ -th hidden features $[\mathbf{h}_{p_1}^{(i+1)}, \mathbf{h}_{e_1}^{(i+1)}, \mathbf{h}_{a_1}^{(i+1)}]$. In addition, an adaptive layer normalization [44] is introduced before each attention and feed-forward layer to incorporate conditioning on the textual signal \mathbf{c} and the timestep t .

4.3. Sparse Interaction Graph

Furthermore, we argue that the FIG exteroception \mathbf{x}_e built from all J joints of each humanoid contradicts the inherently sparse nature of inter-agent relations. For instance, during a handshake, the interaction is primarily governed by the agents’s arms and hands, whereas the lower-body joints contribute minimally to the exchange of interactive behavior dynamics. This indicates that the model should selectively focus on the hand-to-hand relations, where salient

motion cues and inter-agent dependencies emerge.

Sparse attention on interaction graph. To this end, we incorporate a sparse attention mechanism to suppress redundant relations in the FIG exteroception and selectively enhance the most salient inter-agent dependencies. Specifically, the FIG sequence contains $l_e * J * J$ edges, where l_e is the FIG sequence length. These edges are evenly partitioned into subsets, each handled by a distinct attention head. Each head computes the attention logit between its corresponding queries and the assigned edges. Mathematically, a feature sequence $\mathbf{f} \in \mathbb{R}^{l_f \times d_f}$ is input as a query source, where l_f denotes the length of the feature sequence, d_f represents the dimension of the features. The query projection layer projects \mathbf{f} to a query $\mathbf{Q} = \mathbf{f} \cdot \mathbf{W}^Q$, where $\mathbf{W}^Q \in \mathbb{R}^{d_f \times d_f}$. And the reshaped FIG edges $\mathbf{x}_e \in \mathbb{R}^{(l_e * J * J) \times 3}$ are projected to a key $\mathbf{K} = \mathbf{x}_e \cdot \mathbf{W}^K$, and a value $\mathbf{V} = \mathbf{x}_e \cdot \mathbf{W}^V$, where $\mathbf{W}^K, \mathbf{W}^V \in \mathbb{R}^{3 \times d_f}$. Then we obtain the attention map $\mathbf{A} \in \mathbb{R}^{l_f \times (l_e * J * J)}$ with the Gumble-Softmax [13, 87]:

$$\mathbf{A} = \text{Gumble-Softmax}\left(\frac{\mathbf{Q}\mathbf{K}^T}{\sqrt{d_f}}\right). \quad (4)$$

Next, we derive a binary mask \mathbf{M} to retain the most significant edges with the high scores, while filtering out the rest to enforce structural sparsity.

$$\mathbf{M}_{ij} = \begin{cases} 1, & j \in \arg \text{TopK}_k(\mathbf{A}_i) \\ 0, & \text{otherwise} \end{cases}, \quad (5)$$

where $\arg \text{TopK}_k(\cdot)$ denotes the indices corresponding to the top- k columns of \mathbf{A}_i ranked by its values, \mathbf{A}_i is the i -th row of \mathbf{A} . Finally, we can get the output \mathbf{f}' with the following attention mechanism:

$$\mathbf{f}' = (\mathbf{M} \circ \mathbf{A})\mathbf{V}, \quad (6)$$

where \circ denotes the Hadamard product. To highlight the inherently sparse structure, the full connected IG in Eq. (2), after processing through Eqs. (4), (5), and (6), is denoted as the Sparse IG (SIG) for clarity.

5. Experiments

5.1. Experiment Setup

Dataset and evaluation metrics. We evaluate our model on the InterHuman [32] dataset. It is a multi-human MoCap dataset with fine-grained text annotations, widely used as multi-human generation benchmark. We follow the commonly adopted evaluation protocol in the text-to-motion literature, which consists of five metrics: (1) *R-Precision* measures text–motion consistency via motion-to-text retrieval accuracy. (2) *Fréchet Inception Distance (FID)* quantifies the distributional gap between generated and real motions. (3) *Multimodal Distance (MMDist)* evaluates the alignment

	R-precision \uparrow			FID \downarrow	MM dist \downarrow	Diversity \rightarrow	MModality \uparrow
	Top 1	Top 2	Top 3				
Phys-GT	0.481 \pm 0.006	0.633 \pm 0.008	0.722 \pm 0.006	0.004 \pm 0.000	3.401 \pm 0.002	2.080 \pm 0.011	-
InterGen++ [32]	0.287 \pm 0.007	0.439 \pm 0.006	0.542 \pm 0.006	0.943 \pm 0.012	3.751 \pm 0.007	2.044 \pm 0.006	2.482 \pm 0.003
InterMask++ [27]	0.156 \pm 0.008	0.259 \pm 0.009	0.339 \pm 0.009	2.143 \pm 0.035	4.027 \pm 0.009	1.974 \pm 0.011	1.939 \pm 0.003
PDP [66]	0.183 \pm 0.006	0.291 \pm 0.007	0.375 \pm 0.009	1.268 \pm 0.151	3.927 \pm 0.010	1.954 \pm 0.021	2.402 \pm 0.013
CLoSD [65]	0.244 \pm 0.008	0.372 \pm 0.009	0.470 \pm 0.005	1.132 \pm 0.020	3.827 \pm 0.008	1.966 \pm 0.008	1.474 \pm 0.005
InterAgent (Ours)	0.375 \pm 0.006	0.525 \pm 0.006	0.615 \pm 0.007	0.582 \pm 0.018	3.585 \pm 0.007	2.018 \pm 0.008	1.903 \pm 0.014

Table 1. Comparison of text-driven physics-based multi-agent control on the InterHuman [32] test set, where \pm indicates 95% confidence interval and \rightarrow / \uparrow / \downarrow means the closer / larger / smaller the better. **Bold** indicates best results.

between text and its corresponding motion in the latent space. (4) *Diversity* measures the variability across different generated motions. (5) *Multimodality* (*MModality*) assesses the variation among motions generated from the same text prompt. To compute these metrics, we train a motion encoder and a text encoder with a contrastive loss, mapping paired text–interaction samples to a shared latent space.

Implementation details. We implement InterAgent using 4 multi-stream DiT blocks, each with a latent dimension of 768. Every block is composed of 1 inter-stream fusion attention, 5 context-aware conditioning attention layers, and 3 independent linear projection layers. The prediction horizon is set to $m = 4$, and the history buffer size to $h = 364$. In practice, we uniformly downsample the first 360 frames in the history buffer to 12 frames and concatenate them with the most recent 4 frames, forming our history state input to the model. We adopt a frozen CLIP-ViT-L/14 model [49] as the text encoder. We further apply classifier-free guidance [20], where 10% of the CLIP embeddings are randomly masked to zero during training, and a guidance scale of 3.5 is used during sampling. All models are trained using AdamW [38] optimizer with $\beta_1 = 0.9$, $\beta_2 = 0.999$, a weight decay of 2×10^{-5} , and a maximum learning rate of 1×10^{-4} . We employ a cosine learning rate schedule with 5K warm-up iterations and train the model for 80K iterations with a batch size of 256 on 8 NVIDIA GeForce RTX 4090 GPUs, taking approximately 12 hours in total.

5.2. Comparison

We compare our method with four baselines. InterGen++ first generates kinematic motion trajectories from text using InterGen [32] and then employs tracking policy follow the generated trajectory to produce physically plausible motions. InterMask++ follows the same pipeline but replaces the kinematic generator with InterMask [27]. CLoSD [65] and PDP [66] are autoregressive text-to-motion models, which we extend to handle two-person interactions for comparison. As shown in Tab. 1 and Fig. 5, our model achieves superior text–motion alignment and overall realism compared to all baselines, while maintaining

Exteroception	Num. of DiT stream	R-precision (Top-3) \uparrow	FID \downarrow
RS	3	0.588 \pm 0.007	0.676 \pm 0.022
	1	0.523 \pm 0.016	0.828 \pm 0.031
FIG	2	0.608 \pm 0.007	0.662 \pm 0.013
	3	0.612 \pm 0.010	0.634 \pm 0.014
SIG (Ours)	3	0.615 \pm 0.007	0.582 \pm 0.018

Table 2. Quantitative evaluation of the stream number of multi-stream blocks and different exteroception representations.

strong physical plausibility. Although slightly lower than InterGen [32] in Diversity and Multimodality, it consistently outperforms other methods across the remaining metrics. Qualitatively, kinematic–tracking approaches (InterGen++ and InterMask++) often fail to complete full motions or exhibit instability, and autoregressive extensions of CLoSD [65] and PDP [66] tend to miss fine-grained interaction details. In contrast, our method produces physically coherent and semantically faithful interactions—such as a tightly aligned “*hug*” or a precisely targeted “*punch towards the abdomen*”—demonstrating its ability to generate realistic and contextually accurate two-agent motions.

5.3. Ablation Study

Effect of different exteroceptions. To validate the effectiveness of our proposed SIG, we train variants with different exteroceptions (Rows 1, 4, and 5 in Tab. 2). Both FIG and SIG outperform RS in FID and R-precision, showing that interaction graphs yield more structured and informative inter-agent representations. Moreover, our SIG achieves lower FID and higher R-precision than FIG, indicating that its sparse attention effectively exploits the inherent sparsity of IG. Qualitative results (Fig. 6, Columns 1, 4, and 5) further confirm that SIG produces more natural and accurate interactive behaviors.

Effect of multi-stream DiT block. To evaluate the multi-stream design of Inter-DiT, we compare it with a single-stream DiT variant that predicts proprioception, exterocep-

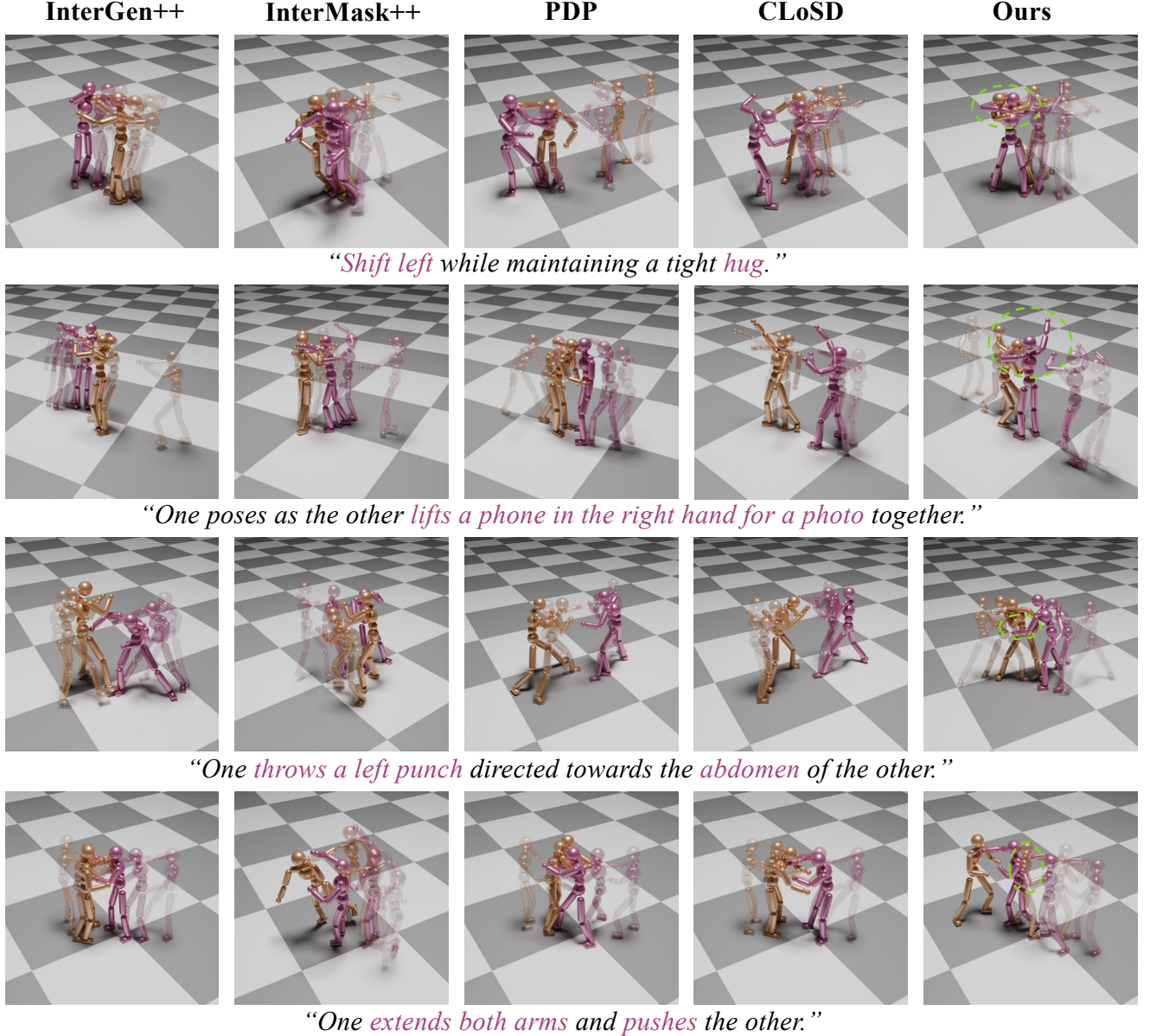


Figure 5. **Qualitative comparison.** Our InterAgent generates more coherent and natural multi-agent interactions that closely align with the given text commands, outperforming all baselines.

tion, and action jointly, and a dual-stream variant that predicts state (proprioception and exteroception) and action separately. As shown in Tab. 2 (Rows 2, 3, and 4) and Fig. 6 (Columns 2, 3, and 4), our triple-stream Inter-DiT consistently outperforms both alternatives across evaluation metrics and qualitative visualizations, demonstrating the effectiveness of the decoupled architecture.

Effect of IG attention and sparsity ratios. We further investigate different sparsity strategies by varying IG attention and sparsity ratios, with edge-based targeting individual joint-to-joint edges and joint-based treating all edges in-

cident to a joint as a single unit. Results (Tab. 3) show that edge-based IG attention with a 1/2 ratio achieves the best performance, indicating that selectively removing less relevant edges more effectively captures inter-agent dependencies while mitigating redundancy, thus improving representation efficiency without sacrificing key relational cues.

5.4. Reactive Humanoid Control

InterAgent enables reactive humanoid control without the need for retraining by incorporating an inpainting mechanism [32, 64, 85] during inference. Specifically, we fix the

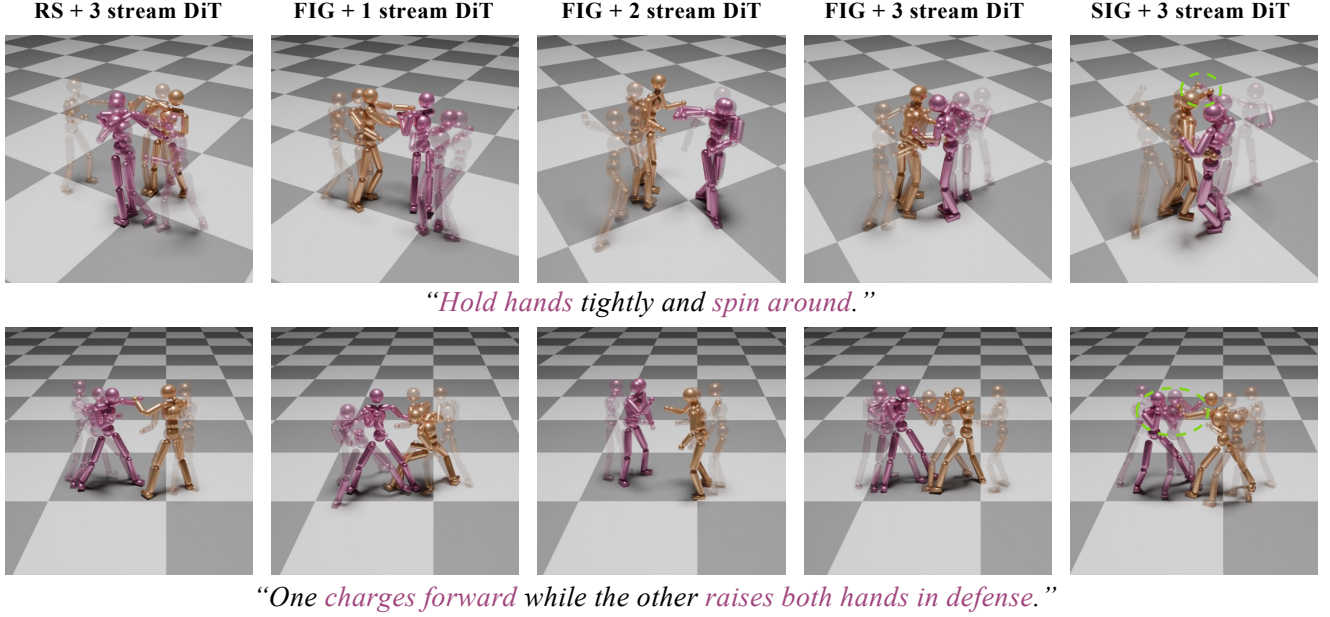


Figure 6. **Ablation study.** We qualitatively evaluate how varying the number of streams in the multi-stream blocks and using different exteroception representations affect the quality and coherence of the generated multi-agent interactions.

IG Attention	Sparsity Ratio	R-precision (Top-3) \uparrow	FID \downarrow
non-sparse	-	0.612 ± 0.010	0.634 ± 0.014
edge-based	3/4	0.609 ± 0.006	0.617 ± 0.026
	1/2	0.615 ± 0.007	0.582 ± 0.018
	1/4	0.602 ± 0.010	0.624 ± 0.026
	1/8	0.601 ± 0.008	0.643 ± 0.020
joint-based	3/4	0.608 ± 0.010	0.615 ± 0.022
	1/2	0.615 ± 0.011	0.619 ± 0.021
	1/4	0.607 ± 0.010	0.591 ± 0.020
	1/8	0.609 ± 0.012	0.603 ± 0.011

Table 3. Quantitative analysis of the IG attention and the effect of different sparsity ratios.

behaviors of one agent via replay, and at each timestep t of the denoising process, after predicting the clean trajectory, we overwrite the fixed agent’s predicted proprioception with its ground truth to guide the generation of responsive behaviors. The visualization results are presented in Fig. 7, where the golden humanoid denotes the fixed behaviors and the pink one represents the text-conditioned generated response. The results demonstrate that our model is capable of synthesizing a diverse repertoire of reaction that are closely adhere to the given textual commands.

6. Conclusion

In this paper, we presented InterAgent, a novel physics-based framework for text-driven multi-agent humanoid con-

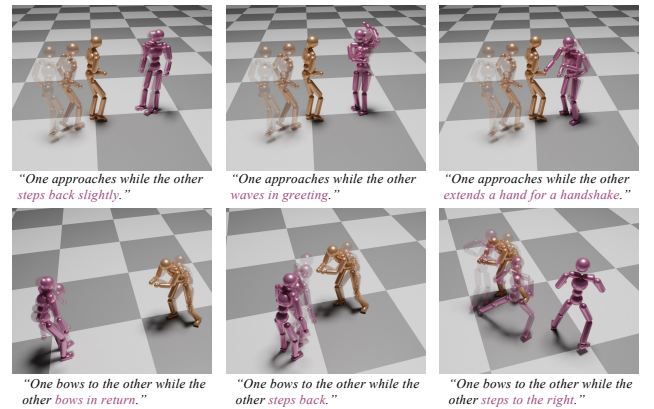


Figure 7. **Reactive humanoid control.** We demonstrate reactive multi-agent control, in which one agent’s motion (gold) is fixed while the other (pink) generates text-conditioned reactions.

trol. By introducing multi-stream DiT architecture, interaction graph exteroception, and the tailored edge-based sparse attention mechanism, our approach effectively models fine-grained inter-agent dependencies while preserving physically plausible and dynamically coherent behaviors. Comprehensive quantitative and qualitative evaluations demonstrate that InterAgent consistently outperforms all baselines in coordinated and physically realistic text-driven multi-agent humanoid control. We firmly believe it can establish a solid foundation for future research in physics-based multi-agent humanoid control and open avenues for broad

applications in gaming, VR/AR, and autonomous robots.

7. Acknowledgement

This work was supported by Shanghai Local College Capacity Building Program (23010503100), NSFC (No.62406195, W2431046, W2431046), Shanghai Frontiers Science Center of Human-centered Artificial Intelligence (ShangHAI), MoE Key Laboratory of Intelligent Perception and Human-Machine Collaboration (ShanghaiTech University), the Shanghai Frontiers Science Center of Human-centered Artificial Intelligence, HPC Platform and Core Facility Platform of Computer Science and Communication of ShanghaiTech University and Shanghai Engineering Research Center of Intelligent Vision and Imaging.

References

- [1] Rick Akkerman, Haiwen Feng, Michael J Black, Dimitrios Tzionas, and Victoria Fernández Abrevaya. Interdyn: Controllable interactive dynamics with video diffusion models. In *Proceedings of the Computer Vision and Pattern Recognition Conference*, pages 12467–12479, 2025. 2
- [2] Zhongang Cai, Jianping Jiang, Zhongfei Qing, Xinying Guo, Mingyuan Zhang, Zhengyu Lin, Haiyi Mei, Chen Wei, Ruisi Wang, Wanqi Yin, et al. Digital life project: Autonomous 3d characters with social intelligence. In *Proceedings of the IEEE/CVF conference on computer vision and pattern recognition*, pages 582–592, 2024. 1
- [3] Jinkun Cao, Jingyuan Liu, Kris Kitani, and Yi Zhou. Multimodal diffusion for hand-object grasp generation. *arXiv preprint arXiv:2409.04560*, 2024. 2
- [4] Zhi Cen, Huaijin Pi, Sida Peng, Qing Shuai, Yujun Shen, Hujun Bao, Xiaowei Zhou, and Ruizhen Hu. Ready-to-react: Online reaction policy for two-character interaction generation. *arXiv preprint arXiv:2502.20370*, 2025. 2
- [5] Rui Chen, Mingyi Shi, Shaoli Huang, Ping Tan, Taku Komura, and Xuelin Chen. Taming diffusion probabilistic models for character control. In *ACM SIGGRAPH 2024 Conference Papers*, pages 1–10, 2024. 2
- [6] Cheng Chi, Zhenjia Xu, Siyuan Feng, Eric Cousineau, Yilun Du, Benjamin Burchfiel, Russ Tedrake, and Shuran Song. Diffusion policy: Visuomotor policy learning via action diffusion. *The International Journal of Robotics Research*, page 02783649241273668, 2023. 1
- [7] Cheng Chi, Zhenjia Xu, Siyuan Feng, Eric Cousineau, Yilun Du, Benjamin Burchfiel, Russ Tedrake, and Shuran Song. Diffusion policy: Visuomotor policy learning via action diffusion. *The International Journal of Robotics Research*, 44(10-11):1684–1704, 2025. 2
- [8] Baptiste Chopin, Hao Tang, Naima Otterdout, Mohamed Daoudi, and Nicu Sebe. Interaction transformer for human reaction generation. *IEEE Transactions on Multimedia*, 25: 8842–8854, 2023. 2
- [9] Sammy Christen, Shreyas Hampali, Fadime Sener, Edoardo Remelli, Tomas Hodan, Eric Sauser, Shugao Ma, and Bugra Tekin. Diffh2o: Diffusion-based synthesis of hand-object interactions from textual descriptions. In *SIGGRAPH Asia 2024 Conference Papers*, pages 1–11, 2024. 2
- [10] Stelian Coros, Philippe Beaudoin, and Michiel Van de Panne. Generalized biped walking control. *ACM Transactions On Graphics (TOG)*, 29(4):1–9, 2010. 2
- [11] Jieming Cui, Tengyu Liu, Nian Liu, Yaodong Yang, Yixin Zhu, and Siyuan Huang. Anyskill: Learning open-vocabulary physical skill for interactive agents. In *Proceedings of the IEEE/CVF conference on computer vision and pattern recognition*, pages 852–862, 2024. 2
- [12] Jieming Cui, Tengyu Liu, Ziyu Meng, Jiale Yu, Ran Song, Wei Zhang, Yixin Zhu, and Siyuan Huang. Grove: A generalized reward for learning open-vocabulary physical skill. In *Proceedings of the Computer Vision and Pattern Recognition Conference*, pages 15781–15790, 2025. 1, 2
- [13] Lingwei Dang, Yongwei Nie, Chengjiang Long, Qing Zhang, and Guiqing Li. Diverse human motion prediction via gumbel-softmax sampling from an auxiliary space. In *Proceedings of the 30th ACM international conference on multimedia*, pages 5162–5171, 2022. 5
- [14] Prafulla Dhariwal and Alexander Nichol. Diffusion models beat gans on image synthesis. *Advances in neural information processing systems*, 34:8780–8794, 2021. 2
- [15] Patrick Esser, Sumith Kulal, Andreas Blattmann, Rahim Entezari, Jonas Müller, Harry Saini, Yam Levi, Dominik Lorenz, Axel Sauer, Frederic Boesel, et al. Scaling rectified flow transformers for high-resolution image synthesis. In *Forty-first international conference on machine learning*, 2024. 4
- [16] Ke Fan, Junshu Tang, Weijian Cao, Ran Yi, Moran Li, Jingyu Gong, Jiangning Zhang, Yabiao Wang, Chengjie Wang, and Lizhuang Ma. Freemotion: A unified framework for number-free text-to-motion synthesis. In *European Conference on Computer Vision*, pages 93–109. Springer, 2024. 1, 2
- [17] Levi Fussell, Kevin Bergamin, and Daniel Holden. Super-track: Motion tracking for physically simulated characters using supervised learning. *ACM Transactions on Graphics (TOG)*, 40(6):1–13, 2021. 2
- [18] Jiawei Gao, Ziqin Wang, Zeqi Xiao, Jingbo Wang, Tai Wang, Jinkun Cao, Xiaolin Hu, Si Liu, Jifeng Dai, and Jiangmiao Pang. Coohei: Learning cooperative human-object interaction with manipulated object dynamics. *Advances in Neural Information Processing Systems*, 37: 79741–79763, 2024. 2
- [19] Tairan He, Jiawei Gao, Wenli Xiao, Yuanhang Zhang, Zi Wang, Jiashun Wang, Zhengyi Luo, Guanqi He, Nikhil Sobanbab, Chaoyi Pan, et al. Asap: Aligning simulation and real-world physics for learning agile humanoid whole-body skills. *arXiv preprint arXiv:2502.01143*, 2025. 2
- [20] Jonathan Ho and Tim Salimans. Classifier-free diffusion guidance. In *NeurIPS 2021 Workshop on Deep Generative Models and Downstream Applications*, 2021. 6
- [21] Jonathan Ho, Ajay Jain, and Pieter Abbeel. Denoising diffusion probabilistic models. *Advances in neural information processing systems*, 33:6840–6851, 2020. 2

- [22] Jessica K Hodgins, Wayne L Wooten, David C Brogan, and James F O'Brien. Animating human athletics. In *Proceedings of the 22nd annual conference on Computer graphics and interactive techniques*, pages 71–78, 1995. 2
- [23] Xiaoyu Huang, Yufeng Chi, Ruofeng Wang, Zhongyu Li, Xue Bin Peng, Sophia Shao, Borivoje Nikolic, and Koushil Sreenath. Diffuseloco: Real-time legged locomotion control with diffusion from offline datasets. *arXiv preprint arXiv:2404.19264*, 2024. 1, 2, 3, 4
- [24] Xiaoyu Huang, Takara Truong, Yunbo Zhang, Fangzhou Yu, Jean Pierre Sleiman, Jessica Hodgins, Koushil Sreenath, and Farbod Farshidian. Diffuse-cloc: Guided diffusion for physics-based character look-ahead control. *ACM Transactions on Graphics (TOG)*, 44(4):1–12, 2025. 2
- [25] Yiming Huang, Zhiyang Dou, and Lingjie Liu. Modskill: Physical character skill modularization. *arXiv preprint arXiv:2502.14140*, 2025. 2
- [26] Michael Janner, Yilun Du, Joshua B Tenenbaum, and Sergey Levine. Planning with diffusion for flexible behavior synthesis. *arXiv preprint arXiv:2205.09991*, 2022. 2
- [27] Muhammad Gohar Javed, Chuan Guo, Li Cheng, and Xingyu Li. Intermask: 3d human interaction generation via collaborative masked modeling. *arXiv preprint arXiv:2410.10010*, 2024. 1, 6
- [28] Jordan Juravsky, Yunrong Guo, Sanja Fidler, and Xue Bin Peng. Padl: Language-directed physics-based character control. In *SIGGRAPH Asia 2022 Conference Papers*, pages 1–9, 2022. 2
- [29] Jordan Juravsky, Yunrong Guo, Sanja Fidler, and Xue Bin Peng. Superpadl: Scaling language-directed physics-based control with progressive supervised distillation. In *ACM SIGGRAPH 2024 Conference Papers*, pages 1–11, 2024. 2
- [30] Minsu Kim, Eunho Jung, and Yoonsang Lee. Physicsfc: Learning user-controlled skills for a physics-based football player controller. *ACM Transactions on Graphics (TOG)*, 44(4):1–21, 2025. 2
- [31] Sergey Levine and Vladlen Koltun. Guided policy search. In *International conference on machine learning*, pages 1–9. PMLR, 2013. 2
- [32] Han Liang, Wenqian Zhang, Wenxuan Li, Jingyi Yu, and Lan Xu. Intergen: Diffusion-based multi-human motion generation under complex interactions. *International Journal of Computer Vision*, 132(9):3463–3483, 2024. 1, 2, 4, 5, 6, 7
- [33] Jacky Liang, Viktor Makoviychuk, Ankur Handa, Nuttapong Chentanez, Miles Macklin, and Dieter Fox. Gpu-accelerated robotic simulation for distributed reinforcement learning. In *Conference on Robot Learning*, pages 270–282. PMLR, 2018. 3
- [34] Binhui Liu, Xin Liu, Anbo Dai, Zhiyong Zeng, Dan Wang, Zhen Cui, and Jian Yang. Dual-stream diffusion net for text-to-video generation. *arXiv preprint arXiv:2308.08316*, 2023. 4
- [35] Libin Liu and Jessica Hodgins. Learning basketball dribbling skills using trajectory optimization and deep reinforcement learning. *Acm transactions on graphics (tog)*, 37(4):1–14, 2018. 2
- [36] Yunze Liu, Changxi Chen, Chenjing Ding, and Li Yi. Phys-reaction: Physically plausible real-time humanoid reaction synthesis via forward dynamics guided 4d imitation. In *Proceedings of the 32nd ACM International Conference on Multimedia*, pages 3771–3780, 2024. 2
- [37] Zihao Liu, Mingwen Ou, Zunnan Xu, Jiaqi Huang, Haonan Han, Ronghui Li, and Xiu Li. Separate to collaborate: Dual-stream diffusion model for coordinated piano hand motion synthesis. In *Proceedings of the 33rd ACM International Conference on Multimedia*, pages 9743–9752, 2025. 4
- [38] Ilya Loshchilov and Frank Hutter. Decoupled weight decay regularization. In *International Conference on Learning Representations*, 2019. 6
- [39] Zhengyi Luo, Ryo Hachiuma, Ye Yuan, and Kris Kitani. Dynamics-regulated kinematic policy for egocentric pose estimation. *Advances in Neural Information Processing Systems*, 34:25019–25032, 2021. 2
- [40] Zhengyi Luo, Jinkun Cao, Josh Merel, Alexander Winkler, Jing Huang, Kris Kitani, and Weipeng Xu. Universal humanoid motion representations for physics-based control. *arXiv preprint arXiv:2310.04582*, 2023. 2, 3
- [41] Zhengyi Luo, Jinkun Cao, Alexander W. Winkler, Kris Kitani, and Weipeng Xu. Perpetual humanoid control for real-time simulated avatars. In *International Conference on Computer Vision (ICCV)*, 2023. 2, 3
- [42] Alexander Quinn Nichol and Prafulla Dhariwal. Improved denoising diffusion probabilistic models. In *International conference on machine learning*, pages 8162–8171. PMLR, 2021. 2
- [43] Liang Pan, Zeshi Yang, Zhiyang Dou, Wenjia Wang, Buzhen Huang, Bo Dai, Taku Komura, and Jingbo Wang. Tokenhsi: Unified synthesis of physical human-scene interactions through task tokenization. In *Proceedings of the Computer Vision and Pattern Recognition Conference*, pages 5379–5391, 2025. 2
- [44] William Peebles and Saining Xie. Scalable diffusion models with transformers. In *Proceedings of the IEEE/CVF international conference on computer vision*, pages 4195–4205, 2023. 5
- [45] Xiaogang Peng, Yiming Xie, Zizhao Wu, Varun Jampani, Deqing Sun, and Huaizu Jiang. Hoi-diff: Text-driven synthesis of 3d human-object interactions using diffusion models. In *Proceedings of the Computer Vision and Pattern Recognition Conference*, pages 2878–2888, 2025. 2
- [46] Xue Bin Peng, Pieter Abbeel, Sergey Levine, and Michiel Van de Panne. Deepmimic: Example-guided deep reinforcement learning of physics-based character skills. *ACM Transactions On Graphics (TOG)*, 37(4):1–14, 2018. 2, 3
- [47] Xue Bin Peng, Ze Ma, Pieter Abbeel, Sergey Levine, and Angjoo Kanazawa. Amp: Adversarial motion priors for stylized physics-based character control. *ACM Transactions on Graphics (ToG)*, 40(4):1–20, 2021. 2, 3
- [48] Xue Bin Peng, Yunrong Guo, Lina Halper, Sergey Levine, and Sanja Fidler. Ase: Large-scale reusable adversarial skill embeddings for physically simulated characters. *ACM Transactions On Graphics (TOG)*, 41(4):1–17, 2022. 2

- [49] Alec Radford, Jong Wook Kim, Chris Hallacy, Aditya Ramesh, Gabriel Goh, Sandhini Agarwal, Girish Sastry, Amanda Askell, Pamela Mishkin, Jack Clark, et al. Learning transferable visual models from natural language supervision. In *International conference on machine learning*, pages 8748–8763. PmLR, 2021. 6
- [50] Davis Rempe, Zhengyi Luo, Xue Bin Peng, Ye Yuan, Kris Kitani, Karsten Kreis, Sanja Fidler, and Or Litany. Trace and pace: Controllable pedestrian animation via guided trajectory diffusion. In *Proceedings of the IEEE/CVF Conference on Computer Vision and Pattern Recognition*, pages 13756–13766, 2023. 2
- [51] Allen Z Ren, Justin Lidard, Lars L Ankile, Anthony Simeonov, Pulkit Agrawal, Anirudha Majumdar, Benjamin Burchfiel, Hongkai Dai, and Max Simchowitz. Diffusion policy policy optimization. *arXiv preprint arXiv:2409.00588*, 2024. 1
- [52] Jiawei Ren, Mingyuan Zhang, Cunjun Yu, Xiao Ma, Liang Pan, and Ziwei Liu. Insactor: Instruction-driven physics-based characters. *Advances in Neural Information Processing Systems*, 36:59911–59923, 2023. 2
- [53] Michele Rocca, Sheldon Andrews, and Kenny Erleben. Policy-space interpolation for physics-based characters. *Proceedings of the ACM on Computer Graphics and Interactive Techniques*, 8(4):1–22, 2025. 1
- [54] Michele Rocca, Sune Darkner, Kenny Erleben, and Sheldon Andrews. Policy-space diffusion for physics-based character animation. *ACM Transactions on Graphics*, 44(3):1–18, 2025. 1
- [55] Pablo Ruiz-Ponce, German Barquero, Cristina Palmero, Sergio Escalera, and José García-Rodríguez. in2in: Leveraging individual information to generate human interactions. In *Proceedings of the IEEE/CVF Conference on Computer Vision and Pattern Recognition*, pages 1941–1951, 2024. 1, 2
- [56] Yonatan Shafir, Guy Tevet, Roy Kapon, and Amit H Bermano. Human motion diffusion as a generative prior. *arXiv preprint arXiv:2303.01418*, 2023. 2
- [57] Yi Shi, Jingbo Wang, Xuekun Jiang, Bingkun Lin, Bo Dai, and Xue Bin Peng. Interactive character control with autoregressive motion diffusion models. *ACM Transactions on Graphics (TOG)*, 43(4):1–14, 2024. 2
- [58] Merkourios Simos, Alberto Silvio Chiappa, and Alexander Mathis. Reinforcement learning-based motion imitation for physiologically plausible musculoskeletal motor control. *arXiv preprint arXiv:2503.14637*, 2025. 2
- [59] Jascha Sohl-Dickstein, Eric Weiss, Niru Maheswaranathan, and Surya Ganguli. Deep unsupervised learning using nonequilibrium thermodynamics. In *International conference on machine learning*, pages 2256–2265. pmlr, 2015. 2
- [60] Jiaming Song, Chenlin Meng, and Stefano Ermon. Denoising diffusion implicit models. *arXiv preprint arXiv:2010.02502*, 2020. 2
- [61] Wenhui Tan, Boyuan Li, Chuhao Jin, Wenbing Huang, Xiting Wang, and Ruihua Song. Think-then-react: Towards unconstrained human action-to-reaction generation. *arXiv preprint arXiv:2503.16451*, 2025. 2
- [62] Mikihiro Tanaka and Kent Fujiwara. Role-aware interaction generation from textual description. In *Proceedings of the IEEE/CVF international conference on computer vision*, pages 15999–16009, 2023. 2
- [63] Chen Tessler, Yifeng Jiang, Erwin Coumans, Zhengyi Luo, Gal Chechik, and Xue Bin Peng. Maskedmanipulator: Versatile whole-body control for loco-manipulation. *arXiv preprint arXiv:2505.19086*, 2025. 2
- [64] Guy Tevet, Sigal Raab, Brian Gordon, Yonatan Shafir, Daniel Cohen-Or, and Amit H Bermano. Human motion diffusion model. *arXiv preprint arXiv:2209.14916*, 2022. 2, 7
- [65] Guy Tevet, Sigal Raab, Setareh Cohan, Daniele Reda, Zhengyi Luo, Xue Bin Peng, Amit H Bermano, and Michiel van de Panne. Cldsd: Closing the loop between simulation and diffusion for multi-task character control. *arXiv preprint arXiv:2410.03441*, 2024. 1, 2, 6
- [66] Takara Everest Truong, Michael Pisen, Zhaoming Xie, and Karen Liu. Pdp: Physics-based character animation via diffusion policy. In *SIGGRAPH Asia 2024 Conference Papers*, pages 1–10, 2024. 1, 2, 3, 6
- [67] Jonathan Tseng, Rodrigo Castellon, and Karen Liu. Edge: Editable dance generation from music. In *Proceedings of the IEEE/CVF conference on computer vision and pattern recognition*, pages 448–458, 2023. 2
- [68] Ashish Vaswani, Noam Shazeer, Niki Parmar, Jakob Uszkoreit, Llion Jones, Aidan N Gomez, Łukasz Kaiser, and Illia Polosukhin. Attention is all you need. *Advances in neural information processing systems*, 30, 2017. 5
- [69] Jiashun Wang, Jessica Hodgins, and Jungdam Won. Strategy and skill learning for physics-based table tennis animation. In *ACM SIGGRAPH 2024 Conference Papers*, pages 1–11, 2024. 2
- [70] Jingbo Wang, Zhengyi Luo, Ye Yuan, Yixuan Li, and Bo Dai. Pacer+: On-demand pedestrian animation controller in driving scenarios. In *Proceedings of the IEEE/CVF Conference on Computer Vision and Pattern Recognition*, pages 718–728, 2024. 2
- [71] Jiashun Wang, Yifeng Jiang, Haotian Zhang, Chen Tessler, Davis Rempe, Jessica Hodgins, and Xue Bin Peng. Hil: Hybrid imitation learning of diverse parkour skills from videos. *arXiv preprint arXiv:2505.12619*, 2025. 2
- [72] Tingwu Wang, Yunrong Guo, Maria Shugrina, and Sanja Fidler. Unicon: Universal neural controller for physics-based character motion. *arXiv preprint arXiv:2011.15119*, 2020. 2
- [73] Yinhuai Wang, Qihan Zhao, Runyi Yu, Hok Wai Tsui, Ailing Zeng, Jing Lin, Zhengyi Luo, Jiwen Yu, Xiu Li, Qifeng Chen, et al. Skillmimic: Learning basketball interaction skills from demonstrations. In *Proceedings of the Computer Vision and Pattern Recognition Conference*, pages 17540–17549, 2025. 2
- [74] Zhenzhi Wang, Jingbo Wang, Yixuan Li, Dahua Lin, and Bo Dai. Intercontrol: Zero-shot human interaction generation by controlling every joint. *Advances in Neural Information Processing Systems*, 37:105397–105424, 2024. 1

- [75] Jungdam Won, Deepak Gopinath, and Jessica Hodgins. Control strategies for physically simulated characters performing two-player competitive sports. *ACM Transactions on Graphics (TOG)*, 40(4):1–11, 2021. 2
- [76] John Won, Kyungmin Lee, Huiwon Jang, Dongyoung Kim, and Jinwoo Shin. Dual-stream diffusion for world-model augmented vision-language-action model. *arXiv preprint arXiv:2510.27607*, 2025. 4
- [77] Qingxuan Wu, Zhiyang Dou, Chuan Guo, Yiming Huang, Qiao Feng, Bing Zhou, Jian Wang, and Lingjie Liu. Text2interact: High-fidelity and diverse text-to-two-person interaction generation. *arXiv preprint arXiv:2510.06504*, 2025. 2
- [78] Shijie Wu, Yihang Zhu, Yunao Huang, Kaizhen Zhu, Jiayuan Gu, Jingyi Yu, Ye Shi, and Jingya Wang. Afforddp: Generalizable diffusion policy with transferable affordance. In *Proceedings of the Computer Vision and Pattern Recognition Conference*, pages 6971–6980, 2025. 1
- [79] Yifan Wu, Zhiyang Dou, Yuko Ishiwaka, Shun Ogawa, Yuke Lou, Wenping Wang, Lingjie Liu, and Taku Komura. Cbil: collective behavior imitation learning for fish from real videos. *ACM Transactions on Graphics (TOG)*, 43(6):1–17, 2024. 2
- [80] Yan Wu, Korrawe Karunratanakul, Zhengyi Luo, and Siyu Tang. Uniphys: Unified planner and controller with diffusion for flexible physics-based character control. *arXiv preprint arXiv:2504.12540*, 2025. 1, 2, 3, 4
- [81] Liang Xu, Xintao Lv, Yichao Yan, Xin Jin, Shuwen Wu, Congsheng Xu, Yifan Liu, Yizhou Zhou, Fengyun Rao, Xingdong Sheng, et al. Inter-x: Towards versatile human-human interaction analysis. In *Proceedings of the IEEE/CVF conference on computer vision and pattern recognition*, pages 22260–22271, 2024. 1, 2
- [82] Liang Xu, Yizhou Zhou, Yichao Yan, Xin Jin, Wenhan Zhu, Fengyun Rao, Xiaokang Yang, and Wenjun Zeng. Regennet: Towards human action-reaction synthesis. In *Proceedings of the IEEE/CVF conference on computer vision and pattern recognition*, pages 1759–1769, 2024. 2
- [83] Sirui Xu, Zhengyuan Li, Yu-Xiong Wang, and Liang-Yan Gui. Interdiff: Generating 3d human-object interactions with physics-informed diffusion. In *Proceedings of the IEEE/CVF International Conference on Computer Vision*, pages 14928–14940, 2023. 2
- [84] Sirui Xu, Hung Yu Ling, Yu-Xiong Wang, and Liang-Yan Gui. Intermimic: Towards universal whole-body control for physics-based human-object interactions. In *Proceedings of the Computer Vision and Pattern Recognition Conference*, pages 12266–12277, 2025. 2
- [85] Xiyan Xu, Sirui Xu, Yu-Xiong Wang, and Liang-Yan Gui. Moreact: Generating reactive motion from textual descriptions. *arXiv preprint arXiv:2509.23911*, 2025. 7
- [86] Han Xue, Jieji Ren, Wendi Chen, Gu Zhang, Yuan Fang, Guoying Gu, Huazhe Xu, and Cewu Lu. Reactive diffusion policy: Slow-fast visual-tactile policy learning for contact-rich manipulation. *arXiv preprint arXiv:2503.02881*, 2025. 1
- [87] Jiancheng Yang, Qiang Zhang, Bingbing Ni, Linguo Li, Jinxian Liu, Mengdie Zhou, and Qi Tian. Modeling point clouds with self-attention and gumbel subset sampling. In *Proceedings of the IEEE/CVF conference on computer vision and pattern recognition*, pages 3323–3332, 2019. 5
- [88] Ling Yang, Zhilong Zhang, Yang Song, Shenda Hong, Runsheng Xu, Yue Zhao, Wentao Zhang, Bin Cui, and Ming-Hsuan Yang. Diffusion models: A comprehensive survey of methods and applications. *ACM computing surveys*, 56(4):1–39, 2023. 2
- [89] Heyuan Yao, Zhenhua Song, Baoquan Chen, and Libin Liu. Controlvae: Model-based learning of generative controllers for physics-based characters. *ACM Transactions on Graphics (TOG)*, 41(6):1–16, 2022. 2
- [90] Heyuan Yao, Zhenhua Song, Yuyang Zhou, Tenglong Ao, Baoquan Chen, and Libin Liu. Moconvq: Unified physics-based motion control via scalable discrete representations. *ACM Transactions on Graphics (TOG)*, 43(4):1–21, 2024. 2
- [91] Wei Yao, Yunlian Sun, Chang Liu, Hongwen Zhang, and Jinhui Tang. Physiinter: Integrating physical mapping for high-fidelity human interaction generation. *arXiv preprint arXiv:2506.07456*, 2025. 2
- [92] Hongwei Yi, Justus Thies, Michael J Black, Xue Bin Peng, and Davis Rempe. Generating human interaction motions in scenes with text control. In *European Conference on Computer Vision*, pages 246–263. Springer, 2024. 2
- [93] KangKang Yin, Kevin Loken, and Michiel Van de Panne. Simbicon: Simple biped locomotion control. *ACM Transactions on Graphics (TOG)*, 26(3):105–es, 2007. 2
- [94] Kangning Yin, Weishuai Zeng, Ke Fan, Minyue Dai, Zirui Wang, Qiang Zhang, Zheng Tian, Jingbo Wang, Jiangmiao Pang, and Weinan Zhang. Unitracker: Learning universal whole-body motion tracker for humanoid robots. *arXiv preprint arXiv:2507.07356*, 2025. 2
- [95] Runyi Yu, Yinhuai Wang, Qihan Zhao, Hok Wai Tsui, Jingbo Wang, Ping Tan, and Qifeng Chen. Skillmimic-v2: Learning robust and generalizable interaction skills from sparse and noisy demonstrations. In *Proceedings of the Special Interest Group on Computer Graphics and Interactive Techniques Conference Conference Papers*, pages 1–11, 2025. 2
- [96] Ye Yuan, Jiaming Song, Umar Iqbal, Arash Vahdat, and Jan Kautz. Physdiff: Physics-guided human motion diffusion model. In *Proceedings of the IEEE/CVF international conference on computer vision*, pages 16010–16021, 2023. 1, 2
- [97] Yunbo Zhang, Deepak Gopinath, Yuting Ye, Jessica Hodgins, Greg Turk, and Jungdam Won. Simulation and re-targeting of complex multi-character interactions. In *ACM SIGGRAPH 2023 Conference Proceedings*, pages 1–11, 2023. 2, 3, 4, 1
- [98] Ziyu Zhang, Sergey Bashkirov, Dun Yang, Michael Taylor, and Xue Bin Peng. Add: Physics-based motion imitation with adversarial differential discriminators. *arXiv preprint arXiv:2505.04961*, 2025. 1
- [99] Yi Zhou, Connelly Barnes, Jingwan Lu, Jimei Yang, and Hao Li. On the continuity of rotation representations in neural networks. In *Proceedings of the IEEE/CVF conference*

- on computer vision and pattern recognition*, pages 5745–5753, 2019. [4](#)
- [100] Minjie Zhu, Yichen Zhu, Jinming Li, Junjie Wen, Zhiyuan Xu, Ning Liu, Ran Cheng, Chaomin Shen, Yaxin Peng, Feifei Feng, et al. Scaling diffusion policy in transformer to 1 billion parameters for robotic manipulation. In *2025 IEEE International Conference on Robotics and Automation (ICRA)*, pages 10838–10845. IEEE, 2025. [1](#)
- [101] Qingxu Zhu, He Zhang, Mengting Lan, and Lei Han. Neural categorical priors for physics-based character control. *ACM Transactions on Graphics (TOG)*, 42(6):1–16, 2023. [2](#)

InterAgent: Physics-based Multi-agent Command Execution via Diffusion on Interaction Graphs

Supplementary Material

8. Demo Video

Beyond the qualitative snapshots, we provide a demo video offering more detailed visualizations, further showcasing the effectiveness of our approach.

9. Additional Implementation Details

Interaction tracking policy. To ensure the collected data accurately captures the ongoing interactions among agents, we integrate the interaction graph reward [97] into the training of the tracking policy. Specifically, during the data collection phase, we define each edge of the interaction graph as $e_{ij} = (\mathbf{p}_{ij}, \mathbf{v}_{ij})$, where \mathbf{p}_{ij} and \mathbf{v}_{ij} denote the relative position and relative velocity between joint i and joint j , respectively. Based on this edge representation, we further define the discrepancy for each pair of edges as:

$$d_{pos} = \sum_{i,j \in E} \omega_{ij} \|\mathbf{p}_{ij}^{ref} - \mathbf{p}_{ij}^{sim}\|, \quad (7)$$

$$d_{vel} = \sum_{i,j \in E} \gamma_{ij} \|\mathbf{v}_{ij}^{ref} - \mathbf{v}_{ij}^{sim}\|, \quad (8)$$

where the superscripts *ref* and *sim* correspond to the reference motion and simulation motion, ω_{ij} and γ_{ij} are edge weighting functions detailed in Zhang et al. [97]. Accordingly, we formulate the interaction graph reward as follows:

$$r_{ig} = \exp(-\lambda_{pos} * d_{pos} - \lambda_{vel} * d_{vel}), \quad (9)$$

The root reward is defined as:

$$r_{root} = \exp(-\lambda_{root} * \|\mathbf{x}_{root}^{ref} - \mathbf{x}_{root}^{sim}\|), \quad (10)$$

where the λ_{pos} , λ_{vel} and λ_{root} denote the term sensitivities, \mathbf{x}_{root} represents the position, velocity, orientation and angular velocity of the root joint. Therefore, our reward function is then calculated as:

$$r = r_{ig} * r_{root}. \quad (11)$$

Reactive humanoid control. To enable reactive behaviors, we embed an inpainting mechanism within the inference process. For a given command c , we fix the behaviors of a humanoid via replaying its ground truth. At each denoising step t , upon the model predicting the clean behaviors $\hat{\mathbf{X}} = [\hat{\mathbf{x}}_{p_1}, \hat{\mathbf{x}}_{e_1}, \hat{\mathbf{x}}_{a_1}, \hat{\mathbf{x}}_{p_2}, \hat{\mathbf{x}}_{e_2}, \hat{\mathbf{x}}_{a_2}]$, we substitute the generated proprioception of the fixed humanoid with its ground truth equivalents. For concreteness, we

	Floating ↓ [mm]	Skating ↓ [mm]	Jerk ↓ [mm/frame ³]
Phys-GT	49.92	4.07×10^{-6}	16.24
InterGen++ [32]	53.35	1.24×10^{-3}	12.56
InterMask++ [27]	151.34	4.29×10^{-4}	39.15
PDP [66]	<u>49.84</u>	7.49×10^{-4}	1.98
CLOSD [65]	48.64	2.62×10^{-5}	29.07
InterAgent (Ours)	49.85	<u>2.81×10^{-4}</u>	<u>2.69</u>

Table 4. Quantitative evaluation of physical correctness. **Bold** and underline indicate the best and the second best result.

assume this substitution targets $\hat{\mathbf{x}}_{p_1}$ here, yielding $\hat{\mathbf{X}}' = [\mathbf{x}_{p_1}, \hat{\mathbf{x}}_{e_1}, \hat{\mathbf{x}}_{a_1}, \hat{\mathbf{x}}_{p_2}, \hat{\mathbf{x}}_{e_2}, \hat{\mathbf{x}}_{a_2}]$, which is then used to advance to the subsequent sampling process. This ensures that the generated interaction dynamics strictly constrained by the fixed humanoid’s behaviors. Empirically, we refrain from replacing generated actions with ground truth counterparts, as the intrinsic randomness of simulation environment makes it difficult for the humanoid to maintain balance when the actions in collected dataset are directly deployed.

10. Additional Experimental Results

In this section, we introduce experimental results that are not included in the main paper due to space limit.

Qualitative results. As shown in Fig. 8, We show additional qualitative results generated by our model given various textual commands.

Quantitative physical analysis. To evaluate the physical correctness, we analyze three widely used metrics [80, 96]: *Floating* (measuring vertical drift), *Skating* (indicating horizontal sliding), and *Jerk* (quantifying the smoothness of the motion). Penetration is not reported herein, as it is negligible across all physics-based methods. As shown in Tab. 4, InterMask++ [27] exhibits significantly poor performance in floating and jerk metrics. Such deficiencies make it inherently challenging for humanoids to maintain balance in physical environments, let alone execute complex interactive behaviors. Consequently, such physical inconsistencies directly contribute to its poor FID and R-precision scores. In contrast, Our InterAgent demonstrates competitive performance across all three physical metrics, closely approaching the ground truth (Phys-GT) and outperforming most baseline methods. It strikes a strong balance between minimizing floating, controlling skating, and reducing jerk, making it robust for text-driven physics-based multi-agent humanoid control.

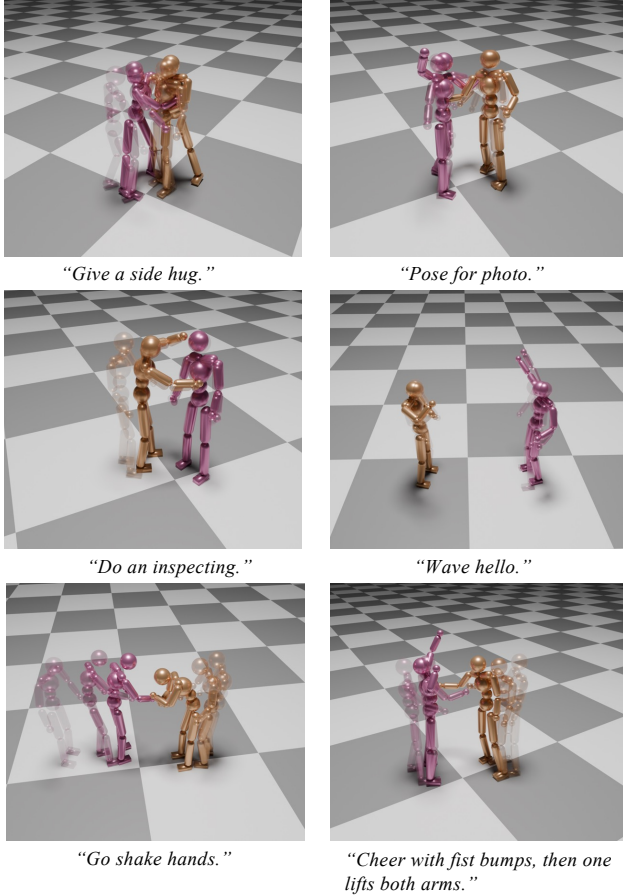


Figure 8. **Qualitative results.**

11. Discussion

Limitations and failure cases. As shown in Fig. 9, our method performs well for most cases but still struggles with more dynamic behaviors like jumping. This issue mainly due to model’s bias toward smooth transitions, which conflicts with the significant instantaneous dynamics of jumping (explosive push-off, mid-air balance, landing impact). A potential solution could involve a dynamic physical constraint module tailored to high-dynamic behaviors. Additionally, augmenting training data with annotated high-dynamic sequences may further enhance the model’s adaptability while preserving its steady-state performance.

Discussion and future work. While InterAgent demonstrates strong capability in generating coordinated, physically plausible, and text-consistent multi-agent behaviors, several aspects of the framework present valuable opportunities for further advancement. Firstly, the current text interface describes high-level motion intent but does not explicitly reason about long-horizon task structure, role assignment, or interactive strategies. Integrating a higher-level planning module, or combining large language mod-

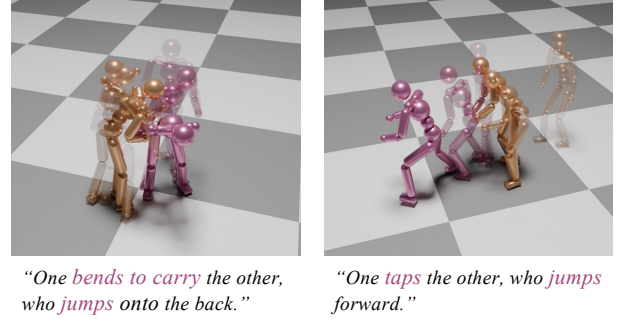


Figure 9. **Failure cases.** Our method struggles with highly dynamic behaviors like jumping.

els with our physics-based controller, could enable richer collaborative behaviors and more natural multi-turn interactions. Secondly, our model is trained with a fixed number of agents, and the computational cost grows with the number of entities due to pairwise relational modeling. Extending the framework toward scalable multi-agent coordination—possibly through hierarchical grouping, clustering of interaction patterns, or dynamic neighborhood selection—will be an essential step toward deployment in complex multi-agent interaction environments. Finally, deploying InterAgent beyond simulation remains an exciting challenge, applying our framework to real humanoid robots or VR/AR avatars will require addressing sim-to-real transfer, real-time inference, and robust perception under noisy sensory inputs. We envision InterAgent serving as a building block for future interactive embodied systems, enabling fluid multi-agent coordination in entertainment, robotics, and immersive virtual environments.